Decadal trends in surface solar radiation and cloud cover over the North Atlantic sector during the last four decades: drivers and physical processes

Climate Dynamics
https://doi.org/10.1007/s00382-022-06438-3

Decadal trends in surface solar radiation and cloud cover over the North Atlantic sector during the last four decades: drivers and physical processes

Buwen Dong[1] · **Rowan T. Sutton**[1] · **Laura J. Wilcox**[1]

Received: 25 February 2022 / Accepted: 21 July 2022

Abstract
Satellite-derived products and reanalyses show consistent increases in downward surface solar radiation (SSR) and decreases in cloud cover over North America and Europe from the 1980s to 2010s. These trends show a strong seasonality, with the largest changes in boreal summer. A set of timeslice experiments with an atmospheric general circulation model (AGCM) forced with prescribed changes in sea surface temperature/sea ice extent (SST/SIE), greenhouse gas (GHG) concentrations, and anthropogenic aerosol (AA) emissions, together and separately, is performed to assess the relative roles of different forcings in these observed trends. The model reproduces the main observed features over Europe and North America, including the seasonality of trends, suggesting a dominant role of forced changes in the recent trends in SSR and cloud cover. Responses to individual forcings indicate that recent decadal trends in SSR over Europe are predominantly driven by AA emission reductions, with an additional influence from SST/SIE and GHG changes. In contrast, changes in AA, SST/SIE, and GHG contribute more equally to simulated decadal trends in SSR and cloud cover over North America, although SST/SIE play the most important role. In our simulations, responses of SSR to AA emission reductions are primarily governed by aerosol-radiation interactions. Responses to SST/SIE and GHG changes are predominantly due to cloud cover changes, which are driven by atmospheric circulation and humidity changes. This process level understanding of how different forcing factors influence decadal trends in SSR and cloud cover is valuable for understanding past changes and future projections in global and regional surface energy budgets, surface warming, and global and regional hydrological cycles.

Keywords Surface solar radiation · Cloud cover · Greenhouse gas concentrations · Anthropogenic aerosol · Sea surface temperature

1 Introduction

Solar radiation is a crucial climate variable and the fundamental energy source for the Earth-atmosphere system. It plays a critical role in driving surface temperatures, large-scale atmospheric circulation, and the global and local hydrological cycle (Allen et al. 2013; Wild et al. 2016; Allan et al. 2020). Downward surface solar radiation (SSR) (also known as downward surface shortwave radiation) represents a major energy exchange at the interface between the atmosphere and the Earth's surface. Changes in SSR therefore have the potential to significantly impact various aspects of the climate system, with associated socio-economic impacts arising from the resultant changes in weather and climate events (Wild 2005; Allen et al. 2013; Wild et al. 2016).

Clouds contribute to Earth's radiation budget through their impacts on shortwave (SW) and longwave (LW) radiation (Stephens et al. 2012) and therefore affect weather and climate (Ramanathan et al. 1989; Boucher et al. 2013). Aerosols can affect SSR directly by radiative absorption and scattering (aerosol-radiation interactions, ARI) (e.g., Boucher et al. 2013; Bellouin et al. 2020) and indirectly by changing cloud characteristics like albedo and lifetime, through their role as cloud condensation nuclei (aerosol-cloud

✉ Buwen Dong
b.dong@reading.ac.uk

[1] National Centre for Atmospheric Science, Department of Meteorology, University of Reading, Reading, UK

Published online: 22 August 2022

interactions, ACI) (e.g., Albrecht 1989; Boucher et al. 2013; Bellouin et al. 2020). Variations in the location and type of aerosol sources as well as their relatively short lifetime give them a high spatiotemporal variability. Consequently, a change in regional aerosol emissions, or a shift of the emission patterns, is expected to affect the local cloud properties and therefore SSR through both ARI and ACI.

During the past few decades, there were large changes in the magnitude and spatial pattern of aerosol and aerosol precursor emissions. These changes are characterized by strong increases from the 1950s to 1970s over North America and Europe, reductions there since the mid-1980s in response to air quality measures, and an increase over Asia and Africa since the 1970s (Klimont et al. 2013). Surface solar radiation measurements in many regions, especially over Europe and North America, have shown large multidecadal swings that have been attributed to these emission changes, with radiation decreases throughout the 1950s–1970s ("dimming") and increases during the 1990s ("brightening") (e.g., Wild et al. 2005; Stjern et al. 2009; Allen et al. 2013; Wild 2016; Schwarz et al. 2020; Wohland et al. 2020; Wang et al. 2022). These observed multidecadal changes likely played an important role in regulating surface warming, and global and regional hydrological cycles (Wild et al. 2005; Wild 2016; Folini and Wild 2011; Allen et al. 2013; Freychet et al. 2019; Allan et al. 2020; Cherian and Quaas 2020).

A number of studies have identified positive trends in SSR, and negative trends in cloud cover over the North Atlantic sector, using satellite-derived products and station observations from 1980s (e.g., Wild 2005; Wild 2016; Norris and Evan 2007; Norris et al. 2016; Allen et al. 2013; Nabat et al. 2014; Sanchez-Lorenzo et al. 2017a, b; Pfeifroth et al. 2018a, b). It has been suggested that anthropogenic forcings, in particular aerosol forcings, are likely to be the dominant factor for these trends (e.g., Ruckstuhl and Norris 2009; Allen et al. 2013; Turnock et al. 2015; Norris et al. 2016; Boers et al. 2017; Freychet et al. 2019; Cherian and Quaas 2020).

Anthropogenic forcings, including greenhouses and aerosols, may affect cloud cover and SSR directly, and indirectly through their influence on sea surface temperature (e.g., Gregory and Andrews 2016; Zhou et al. 2016; Dong et al. 2017). Previous studies have indicated that changes in SSR and cloud cover are important factors in extreme hot temperatures and heatwaves over Europe and North America (e.g., Smith et al. 2013; Dong et al. 2016; 2017; Freychet et al. 2019; Luo et al. 2020; Tang et al. 2020). However, a detailed understanding of how changes in forcings may have affected cloud cover and SSR in the North Atlantic sector during the last four decades is still lacking, especially regarding the relative importance of different forcing factors.

The aim of this study is to quantify the relative roles of different drivers for recent decadal trends in SSR and cloud cover over the North Atlantic sector, and to elucidate mechanisms by performing numerical experiments with an atmospheric General Circulation Model. A specific focus of this study is to assess and quantify relative roles of changes in anthropogenic aerosols (AA), greenhouses gas (GHG) concentrations, and sea surface temperature/sea ice extent (SST/SIE), and to understand the physical processes in response to individual forcings. This process level understanding of how different forcing factors influence decadal changes in SSR and cloud cover is of crucial importance for understanding their future projections and relevant climate impacts.

The rest of the paper is organized as follows: in Sect. 2, the observational/reanalysis data, model, and model experiments used are briefly described. Decadal changes of SSR, cloud cover, and extreme temperatures in boreal summer in observations/reanalyses, model responses to different forcings, and physical processes are documented in Sect. 3. Seasonality of decadal changes in SSR and cloud cover are discussed in Sect. 4, and conclusions are given in Sect. 5.

2 Observations and model experiments

2.1 Observations and reanalyses

We use observations of SSR and cloud fraction from the international satellite cloud climatology project (ISCCP; Rossow and Schiffer 1999). The SSR product is available for 1984–2015 (Norris and Evan 2015), and bias corrected cloud cover is available for 1984–2009. Monthly mean sea surface temperature and sea ice extent (SST/SIE) are taken from HadISST (Rayner et al. 2003). We also use the new state-of-the-art climate reanalysis ERA5 (Hersbach et al. 2020) and NCEP-NCAR reanalysis II (Kanamitsu et al. 2002). Using reanalyses can expand model evaluation to a wider range of variables, including atmospheric circulation variables.

2.2 Model and model experiments

The model used in this study is the Met Office atmosphere and land model GA6.0 (MetUM-GA6, see Walters et al. 2017) with a resolution of 1.875° longitude by 1.25° latitude and 85 levels in the vertical. The model includes prognostic tropospheric aerosol modelling using the CLASSIC (Coupled Large-scale Aerosol Simulator for Studies in Climate) aerosol module, which represents seven tropospheric aerosol species (sulphate, mineral dust, fossil-fuel black carbon, fossil-fuel organic carbon, biomass-burning, sea-salt, and

secondary organic aerosols from biogenic emissions). This aerosol module includes the sulphur cycle with emissions of sulphur dioxide and dimethyl sulphide (DMS) that are prognostic tracers of the atmosphere model and are oxidized into sulphate by the hydroxyl radical, hydrogen peroxide, the peroxide radical and ozone. Emissions for sea-salt and mineral dust aerosols are computed interactively so emission data sets are not required. For most species, aerosol mass is distributed across three model tracers associated with the Aitken, accumulation, and dissolved modes. Both aerosol-radiation interactions (ARI) and aerosol-cloud interactions (ACI) are considered (Bellouin et al. 2011).

As SSR was observed to increase rapidly during the 1990s over Europe and North America (e.g., Wild et al. 2005; Allen et al. 2013; Wild 2016; Schwarz et al. 2020; Wohland et al. 2020; Wang et al. 2022), we chose a baseline period of 1980–1995 and a more recent period of 2000–2015 for our timeslice experiments. There were changes in several potential drivers of climate between these two periods. Sea surface temperatures (SSTs) warmed, with large warming anomalies over the North Atlantic subpolar gyre and over the tropical Indian Ocean and western Pacific (supplementary Fig. S1a, b). There were associated changes in sea-ice extent (SIE), particularly in the Arctic. GHG concentrations also increased due to anthropogenic emissions (CO_2 increased by 9.9%, CH_4 increased by 7.6%, and N_2O increased by 4.6%), and there were significant changes in anthropogenic aerosol (AA) emissions. The changes in annual mean sulphur dioxide emissions, a major aerosol precursor, involve decreases over Europe and North America and increases over East and South Asia (supplementary Fig. S1c). Other important aerosol precursor emissions, such as fossil-fuel black carbon and fossil-fuel organic carbon also show decreases over Europe and North America and increases over East Asia (e.g., Yang et al. 2018a, b; 2020).

A set of 40-year long timeslice experiments was carried out to identify the roles of changes in: (i) global SST/SIE, (ii) prescribed GHG concentrations, and (iii) AA forcings in regulating the changes of SSR and cloud cover over the North Atlantic sector. AA forcings are prescribed aerosol precursor emissions of five species that include sulphur dioxide, fossil-fuel black carbon, fossil-fuel organic carbon, biomass-burning, and secondary organic aerosols from biogenic emissions. The experiments, summarised in Table 1, are: CON experiment forced by the early period (1980–1995) climatological monthly mean SST/SIE, GHGs and AA emissions; ALL experiment forced by the recent period (2000–2015) climatological monthly mean SST/SIE, GHGs and AA emissions; SSTAA experiment forced by the recent period SST/SIE and AA emissions with the early period GHGs; SST experiment forced by the recent period SST/SIE with the early period GHGs and AA emissions. Note that our experimental design assumes a linear addition of responses to different forcing factors. The last 38 years of each experiment are analysed and the response to a particular forcing is estimated by the difference between a pair of experiments that include and exclude that particular forcing. For example, the response to AA forcing is the difference between experiment SSTAA and experiment SST. In this set of experiments, SST/SIE is taken as an independent forcing factor, and responses to changes in GHGs and AA only consider the fast atmospheric and land responses. The main focus of our analysis is on changes in boreal summer (June-August: JJA) since the largest changes in SSR over the Atlantic sector in observations and reanalyses occurred in this season. Seasonality is briefly investigated by analysing seasonal means of December-February (DJF), March-May (MAM), and September-November (SON). Statistical significance of the seasonal mean changes is assessed using a two tailed Student's t-test.

Table 1 Summary of numerical experiments using MetUM-GA6 for recent decadal changes

Experiments	Boundary conditions
CON	Monthly climatological SST and sea ice averaged over period 1980–1995 using HadISST (Rayner et al. 2003) with greenhouse gases (GHGs) concentrations and anthropogenic aerosol (AA) emissions (Lamarque et al. 2010, 2011) averaged over the same period.
ALL	Monthly climatological SST and sea ice averaged over period 2000–2015, with GHGs concentrations and AA emissions over the same period.
SSTAA	As ALL, but with GHGs over period 1980–1995.
SST	As ALL, but with GHGs concentrations and AA emissions averaged over period 1980–1995.

3 Decadal changes of SSR, cloud cover, and extreme temperatures in boreal summer

3.1 Recent trends of SSR and cloud cover in observations

Figure 1 shows time series of SSR and cloud cover anomalies in JJA averaged over North America, North Atlantic and Europe from two reanalyses during 1980–2015 and the ISCCP product during 1984–2015/2009. One of the most prominent features is positive trends in SSR and negative trends in cloud cover over these regions. Different data sets show consistent trends and interannual variations over these regions although SSR trends in ISCCP and ERA5 are larger than those in NCEP2, likely because the NCEP2 reanalysis does not include a time-varying aerosol component. The correlations among three time series are calculated for SSR

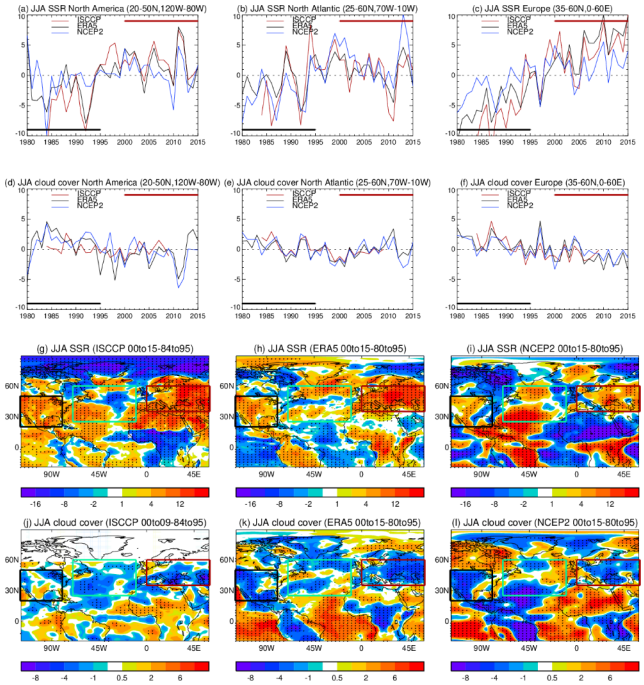

Fig. 1 (a-f) Times series of area averaged downward surface solar radiation (SSR, W m^{-2}), total cloud cover (%) anomalies over North America, North Atlantic, and Europe in JJA based on the ISCCP product, ERA5, and NCEP2 reanalyses. (g-l) spatial patterns of changes between 2000–2015 and 1980–1995. The two horizonal bars in (a-f) highlight periods 1980–1995 and 2000–2015. Dots in (g-l) highlight regions where changes are statistically significant at the 10% level based on a two-tailed Student's t-test. Black, green and red boxes (g-l) highlight regions that used to calculate area averaged values

during 1984–2015 and cloud cover during 1984–2009. They range from 0.60 to 0.90 for SSR over three regions and from 0.58 to 0.87 for cloud cover over North Atlantic and Europe. These correlations are statistically significant at the 5% level based on a two-tailed Student's t-test, indicating consistent variations among three data sets. However, ISCCP cloud cover variations over North America show less consistent variations in comparison with ERA5 or NCEP2 with low correlation coefficients of 0.39 and 0.13 although ERA and NCEP2 variations are more consistent (0.75). These consistent trends and interannual variations indicate robust changes of these two variables during the past four decades, which are physically linked as the reduction in cloud cover causes less solar incoming radiation to be reflected to space, leading to increased SSR. The correlation coefficients between SSR and cloud cover time series for the three datasets are – 0.86, -0.83, -0.91 over Europe, -0.35, -0.77, -0.57 over North America, and – 0.74, -0.84, -0.89 over the North Atlantic, for ISCCP, ERA5, and NCEP2. The weak correlation (-0.35) between SSR and cloud cover variations in ISCCP over North America is due to weak and less consistent cloud variations in this data set in comparison with those in ERA5 and NCEP2. The opposite is true for large correlation (-0.77) in ERA5. Superimposed on the long-term trends are distinct positive SSR anomalies and negative cloud cover anomalies over Europe in 2003, 2010 and 2015 which played a key role in heatwave events in those years (e.g., Otto et al. 2012; Christidis et al. 2015; Dong et al. 2016).

To investigate these trends in greater detail we examine differences between means over two 16-year time periods: 1980–1995 and 2000–2015. The results for JJA are shown in Fig. 1. All three data sets show consistent increases of SSR and decreases of cloud cover over North America and Europe but less consistent changes over the North Atlantic. Quantitatively, consistent and statistically significant positive SSR anomalies are observed over North America (4–6 Wm^{-2}) and over Europe (8–12 Wm^{-2}) in ISCCP and ERA5. The anomalies are smaller in NCEP2 over both regions (Fig. 1g, h, i). These increases in SSR in the three highlighted regions in Fig. 1 are associated with a reduction of cloud cover: a reduction of cloud fraction by 1.5-2.0% over Europe in the three datasets, and similar decreases over North America in ERA5 and NCEP2. The decrease in cloud fraction over North America is weaker in ISCCP, and is less clearly reflected in the SSR changes (Fig. 1j, k, l). However, there is some uncertainty in the SSR anomalies over tropical and subtropical regions where ISCCP and two reanalysis data sets show opposite signs of changes (Fig. 1g-i), resulting a low pattern correlation of 0.25 between ISCCP and ERA5 and 0.23 between ISCCP and NCEP2 in a 2.5°x2.5° common grid over the whole domain.

To show whether the differences of changes between two periods in SSR and cloud cover among different data sets are related to their climatologies, the climatological mean differences between ISCCP and ERA5 datasets in JJA for SSR and cloud cover are shown in supplementary Fig. S2. ISCCP shows 8–16 Wm^{-2} less SSR than ERA5 over North America and the North Atlantic and more cloud cover fraction in the three regions (8–15%) over both periods. These climatological differences between the two data sets are larger than decadal trends between two periods shown in Fig. 1. The spatial patterns of the climatological differences between two datasets also differ from the patterns of decadal trends. Despite these large climatological differences between two data sets, the decadal trends in two data sets show consistent and similar magnitude changes over Europe and North America, especially for SSR. This suggests that differences in the climatologies of the different datasets do not make substantial contributions to difference in the decadal trends in SSR and cloud cover.

The increased SSR and decreased cloud cover over North America and Europe are associated with changes in relative humidity in the lower troposphere and atmospheric circulation over the North Atlantic sector (Fig. 2). The changes in

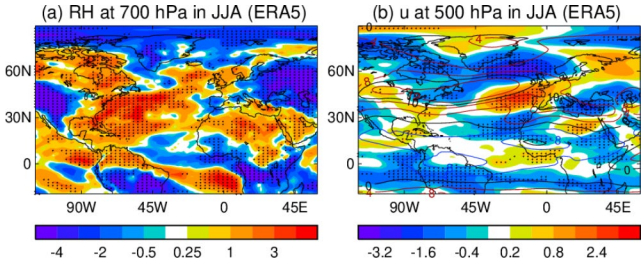

Fig. 2 Changes of (a) relative humidity at 700 hPa (%) and (b) zonal wind at 500 hPa (m s^{-1}) in JJA between 2000-2015 and 1980-1995 based on ERA5 with contours in (b) (red for westerlies and blue for easterlies) showing climatology during 1980–1995. Dots highlight regions where differences are statistically significant at the 10% level based on a two-tailed Student's t-test

relative humidity are characterized by decreases over North America and Europe (Fig. 2a), consistent with the decreases in cloud cover over these two regions. Changes of atmospheric circulation over the North Atlantic show a tripole pattern of zonal wind anomalies indicating a southward displacement of the North Atlantic eddy-driven jet, and a strengthening of the flow into Europe (Fig. 2b). This zonal wind pattern corresponds to decreases of cloud cover over the North Atlantic subpolar region where westerlies are reduced, suggesting an influence of circulation changes on cloud cover over the North Atlantic.

3.2 Model simulated changes in response to different forcing factors

3.2.1 SSR changes

The spatial patterns of SSR changes in ERA5 and model simulated responses to different forcing combinations across the two periods are illustrated in Fig. 3, together with area averaged changes over North America, the North Atlantic, and Europe in both observations/reanalyses and the model simulated responses. The spatial patterns and magnitudes of response to changes in SST/SIE, GHGs, and AA together show some similar features as those in ISCCP and ERA5 with pattern correlations of 0.24 and 0.31, which are similar to pattern correlations among different observation and reanalysis datasets. These low pattern correlations are mainly due to some opposite anomalies in ERA5 and model simulations over the tropics and subtropics where observations/reanalyses also show some large differences. Despite these low pattern correlations, the model simulated responses in SSR are characterized by increases over the North Atlantic sector with large increases over North America and Europe, being similar to changes in ISCCP and ERA5. The large scale patterns of the model simulated changes over the whole domain (Fig. 3) are predominantly due to changes in AA and SST/SIE with pattern correlations

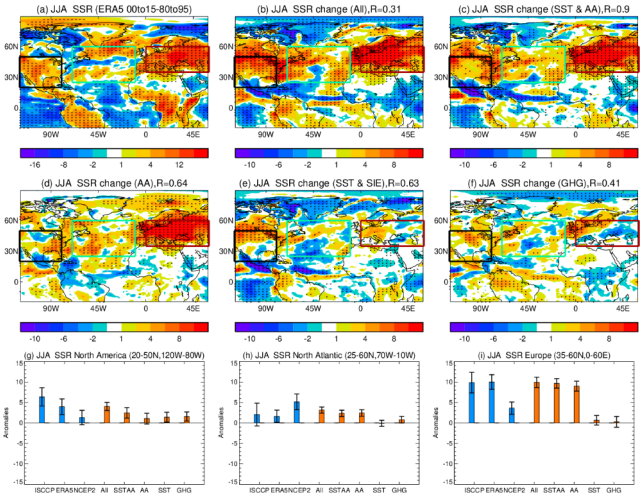

Fig. 3 Spatial patterns of changes in SSR (W m^{-2}) in JJA for (a) ERA5 (same as Fig. 1 h) and for (b-f) responses to different forcings in model experiments. Dots in (a-f) highlight regions where changes are statistically significant at the 10% level based on a two-tailed Student's t-test. R in (b) is the pattern correlation between the all forcing experiment and ERA5 over the whole domain and they are pattern correlations between different forcing experiments and all forcing experiment in (c-f). (g, h, i) area averaged changes over North America, North Atlantic, and Europe (boxes in a-f) between 2000–2015 and 1980–1995 based on the ISCCP product, ERA5, and NCEP2 reanalyses (blue bars) and model responses to different forcings (red bars). Whiskers show 95% uncertainty ranges based on a two-tailed Student's t-test

of 0.90, 0.64, 0.63, and 0.41 between response to all forcings and responses to combined changes in AA and SST/SIE, AA, SST/SIE, and GHGs respectively. Area averaged responses to all forcing in SSR over Europe and North America are 9.9 Wm^{-2} and 4.0 Wm^{-2} respectively, being very close to those of 9.9 Wm^{-2} and 6.4 Wm^{-2} in ISCCP and 10.0 Wm^{-2} and 4.0 Wm^{-2} in ERA5 over the two regions (Fig. 3 g, i, Table 2). Area averaged SSR changes in response to all forcings over Europe and North Atlantic are predominantly due to AA while changes in AA, SST/SIE, and GHGs make comparable contributions to changes over North America with SST/SIE playing a more important role here compared to over Europe (Fig. 3d-f, g-i; Table 2). However, there are some differences in spatial patterns of responses to different forcings. Responses of SSR to all forcings show increased SSR over the North Atlantic (Fig. 3b) with large increases over the western and eastern part, which are largely the result of AA (Fig. 3d). However, responses to SST/SIE show spatial variations over the North Atlantic with increases over the Gulf Stream and its extension and decreases to the south (Fig. 3e). GHG changes induce a dipole pattern of changes in SSR over Europe characterized by increases over north-western Europe and decreases over central and eastern Europe and increases over mid-latitudes around 45°N over eastern North America and over the Gulf Stream (Fig. 3f).

Table 2 Area averaged changes in downward surface solar radiation (SSR, W m^{-2}), total cloud cover (%) over North America, the North Atlantic, and Europe in JJA between 2000–2015 and 1980–1995 based on the ISCCP product, ERA5, and NCEP2 reanalyses and model simulated responses to different forcings all together or separately

	SSR (W m^{-2})			Cloud cover (%)		
	North America	North Atlantic	Europe	North America	North Atlantic	Europe
ISCCP	+6.4	+2.1	+9.9	-0.4	-1.3	-1.8
ERA5	+4.0	+1.6	+10.0	-1.6	-0.5	-2.4
NCEP2	+1.3	+5.2	+3.6	-2.2	-1.0	-1.4
All forcings	+4.0	+3.1	+9.9	-1.4	-0.8	-2.4
AA	+1.1	+2.4	+9.0	+0.6	-0.1	-1.3
SST/SIE	+1.4	-0.1	+0.7	-1.4	-0.2	-1.0
GHG	+1.6	+0.8	+0.3	-0.6	-0.5	-0.1

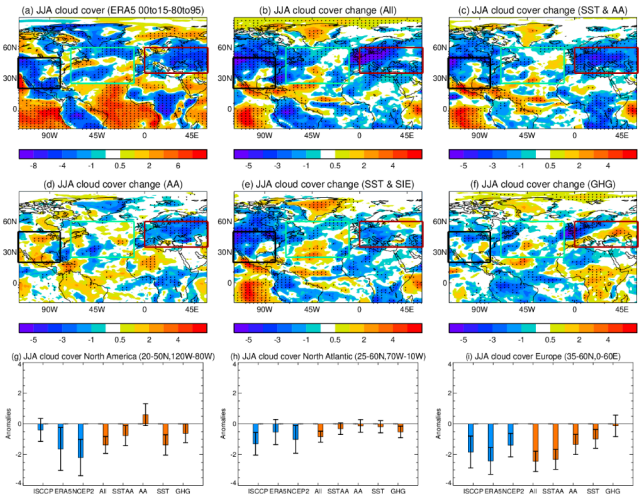

Fig. 4 Spatial patterns of changes in cloud cover (%) in JJA for (a) ERA5 (same as Fig. 1k) and for (b-f) responses to different forcings in model experiments. Dots in (a-f) highlight regions where changes are statistically significant at the 10% level based on a two-tailed Student's t-test. (g, h, i) area averaged changes over North America, North Atlantic and Europe (boxes in a-f) between 2000–2015 and 1980–1995 based on the ISCCP product, ERA5, and NCEP2 reanalyses (blue bars) and model responses to different forcings (red bars). Whiskers show 95% uncertainty ranges based on a two-tailed Student's t-test

3.2.2 Cloud cover changes

Cloud cover changes in the ERA5 reanalysis and model simulations are shown in Fig. 4. The ERA5 reanalysis shows decreases over North America, Europe and over the subpolar region of the North Atlantic (Fig. 4a). In the model, in response to all forcings, cloud cover changes are characterized by a reduction over North America, Europe, and some parts of the North Atlantic (Fig. 4b; Table 2). Over land, model simulated changes are similar to the ERA5 reanalysis, but the model simulates changes of the opposite sign over the Equatorial Atlantic (Fig. 4a, b). Responses to individual forcings contribute to different features of the all-forced response over the North Atlantic sector (Fig. 4c-f, g-h). Reduced cloud cover over North America is predominantly due to changes in SST/SIE with GHG increases a contributing factor (Fig. 4e, f, g; Table 2). In contrast, reduced cloud cover over Europe is largely related to changes in AA with SST/SIE a contributor factor and GHGs leading to a dipole pattern with reduction over northern Europe and increase over the Mediterranean and eastern Europe (Fig. 4d, e, f). Quantitatively, satellite-derived products and reanalyses show a reduction of cloud cover fraction by 1.4–2.4% from 1980s to 2010s over Europe. The model simulates a reduction of 2.4% with AA explaining 54% change and SST/SIE explaining 42% change (Fig. 4i; Table 2).

3.2.3 Clear sky SSR changes and cloud radiative effects

SSR changes are further decomposed into clear sky SSR (Fig. 5) and cloud radiative effect (CRE) related to cloud cover (Fig. 6). ERA5 shows positive clear sky SSR anomalies over the whole domain with large increases over Europe and North America. Over Europe, ISCCP shows a change in SSR of 9.9 Wm^{-2} between two periods of which 68% is due to clear sky and 32% is due to cloud cover while ERA5 shows a change of SSR by 10.0 Wm^{-2} of which 89% is due to clear sky and 11% is related to cloud cover (Figs. 5 and 6). The results indicate that recent SSR increases between 1980-1995 and 2000–2015 in ISCCP and ERA5 over Europe are largely due to increases in clear sky SSR. In response to all forcings, model simulated changes show large positive clear sky SSR anomalies over Europe and North America with weak anomalies in the tropics and subtropics. The model simulated change in SSR (9.9 Wm^{-2}) over Europe is also largely due to the clear sky SSR (5.6 Wm^{-2}). The decrease in cloud cover is responsible for about 4.3 Wm^{-2} SSR change in which changes in AA, SST/SIE, and GHGs are all contributing factors (Fig. 6). SSR change of 9.9 Wm^{-2} in the model response to all forcings over Europe is predominantly due to AA (9.0 Wm^{-2}). 71% of the response to AA is due to changes in clear sky SSR through aerosol-radiation interactions, which closely follow the pattern of changes in aerosol optical depth (AOD, Fig. 7a), and 29% of the response is related to changes in cloud cover (Fig. 6d).

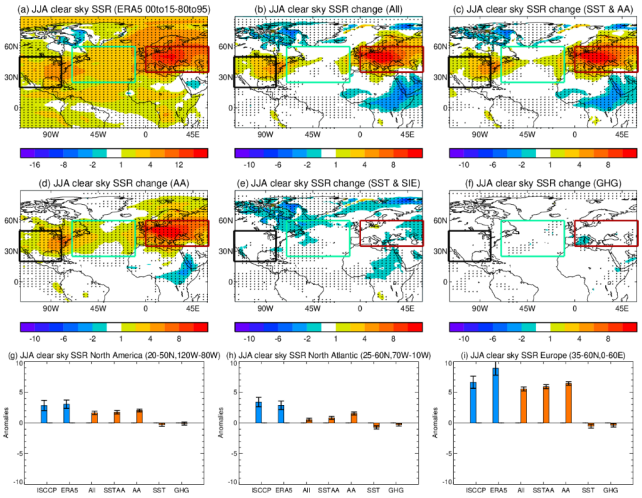

Fig. 5 Spatial patterns of changes in clear sky SSR (W m^{-2}) in JJA for (a) ERA5 and (b-f) responses to different forcings in model experiments. Dots in (a-f) highlight regions where changes are statistically significant at the 10% level based on a two-tailed Student's t-test. (g, h, i) area averaged changes over North America, North Atlantic and Europe (boxes in a-f) between 2000–2015 and 1980–1995 based on the ISCCP product, ERA5 reanalysis (blue bar) and model responses to different forcings (red bar). Whiskers show 95% uncertainty ranges based on a two-tailed Student's t-test

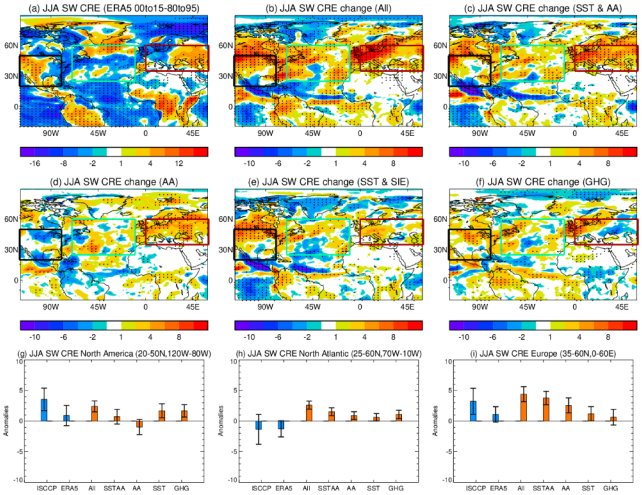

Fig. 6 Spatial patterns of changes in shortwave cloud radiative effect (SW CRE) (W m^{-2}) in JJA for (a) ERA5 and (b-f) responses to different forcings in model experiments. Dots in (a-f) highlight regions where changes are statistically significant at 10% level based on the two-tailed student's t-test. (g, h, i) area averaged changes over North America, North Atlantic and Europe (boxes in a-f) between two periods of 2000–2015 and 1980–1995 based on the ISCCP product, ERA5 reanalysis (blue bar) and model responses to different forcings (red bar). Whiskers show 95% uncertainty ranges based on a two-tailed Student's t-test

These results indicate that changes in SSR over Europe are largely due to changes in clear sky SSR between two periods in both observations and model simulations. The model simulations suggest that changes in AA play a predominant role in these observed changes. These results are consistent with previous studies that suggested changes in cloud cover do not appear to be the dominant factor in driving dimming/brightening trends over Europe (Wild et al. 2005; Norris and Wild 2007; Ruckstuhl and Norris 2009).

Over North America, the clear sky SSR increase in response to all forcings is again due to AA (Fig. 5). However, only SST/SIE and GHGs drive a reduction in cloud cover (Fig. 4), in contrast to Europe where all forcing factors play a role. The SST/SIE and GHGs induced cloud cover reduction makes a large contribution to SSR decrease through CRE (Fig. 6). Another important feature is that SSR increases in response to AA over North America are much weaker (~2.5 Wm^{-2}) than over Europe (9.0 Wm^{-2}). One factor for the weaker response is the smaller changes in AOD over North America compared to Europe (Fig. 7a). Another factor is that cloud changes over North America show some local weak increases, mainly due to small increases in relative humidity. The dominant role of reduced cloud cover on enhanced SSR over North America in the model simulation is in agreement with the study by Augustine and Dutton (2013) who showed observed positive trends in SSR since the 1990s are mainly attributed to decreases in cloud cover. Our results suggest that the recent decadal changes in SST/SIE were the main factors for reduced cloud cover over North America with a contribution from GHG changes. Note that there are differences in patterns between model simulated changes and those in observations over North America and therefore area averaged changes over North America are based on the region which shows large changes in observations.

3.2.4 Attribution of changes in SSR and cloud cover

Results above indicate that recent decadal positive trends in SSR and negative trends in cloud cover over Europe are predominantly driven by AA emission changes while changes over North America were driven largely by changes in SST/SIE, with additional contributions from AA and GHG. The physical processes involved in the response to AA are illustrated in Fig. 7, while those involved in the response to SST/SIE are illustrated in Fig. 8. Reduced aerosol emissions over North America and Europe lead to decreases in AOD over both regions and over the North Atlantic, decreases in cloud droplet number concentration (CDNC), increases in cloud droplet effective radius (CDER) (Fig. 7a, b, c). Decreases in CDNC and increases in CDER are associated with decreased cloud optical depth (e.g., Albrecht 1989; Boucher et al. 2013). The reduced AOD leads to increased clear sky SSR over the North Atlantic sector with large increases over North America and Europe through aerosol-radiation interactions (Fig. 7e). Aerosol reductions also lead to reduced

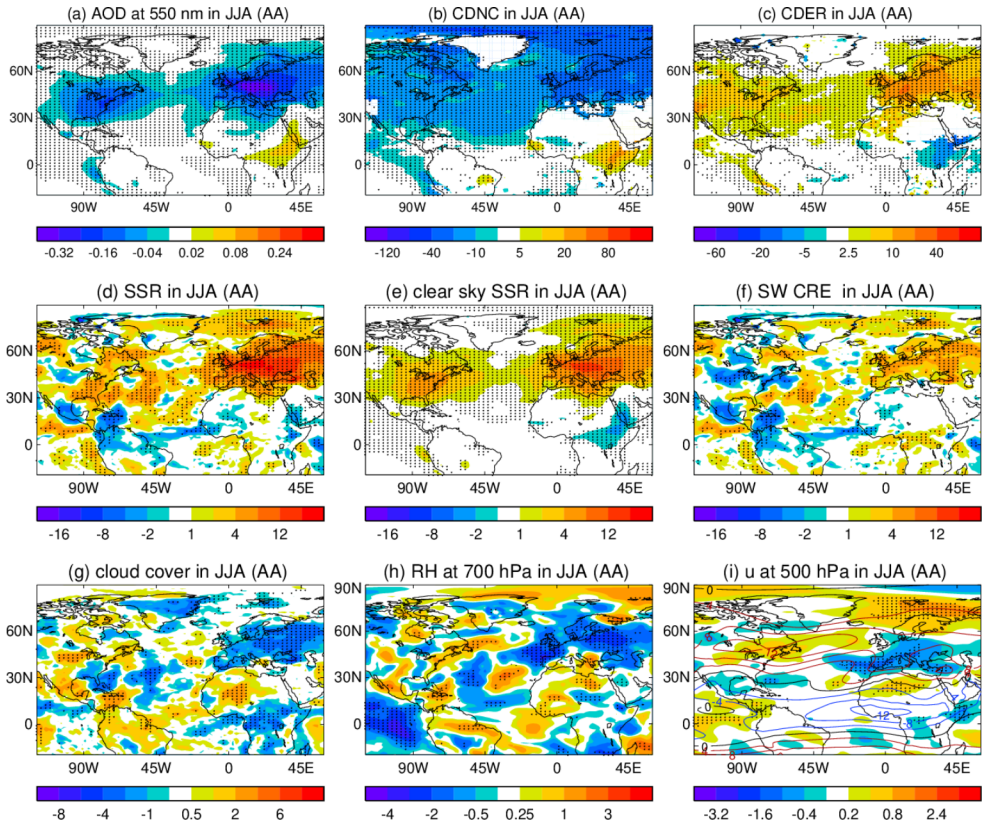

Fig. 7 Simulated seasonal mean responses in JJA to AA emissions changes (SSTAA – SST). (a) AOD at 550 nm, (b) cloud droplet number concentration (CDNC), (c) cloud droplet effective radius (CDER). (d) SSR, (e) clear sky SSR, (f) surface shortwave cloud radiative effect (CRE SW), (g) cloud fraction (%), (h) relative humidity at 700 hPa (%), and (i) zonal wind at 500 hPa (m s^{-1}) with contours (red for westerlies and blue for easterlies) showing climatology in CON. Radiations are positive downwards (W m^{-2}). Changes in CDCN and CDER are percentage changes relative to the experiment CON. Dots highlight regions where differences are statistically significant at the 10% level based on a two-tailed Student's t-test

cloud cover (Fig. 7g), mainly over Europe, where weakened westerlies lead to weakened moisture advection, reduced relative humidity (Fig. 7g, h, i), and reduced evaporation (not shown). The weakened westerlies are caused by reduced surface and low tropospheric meridional temperature gradients over the western Europe induced by non-uniform changes in SSR over the European sector (Dong and Sutton 2021). The reduction in cloud cover further contributes to the increased SSR (Fig. 7d) seen in response to a decrease in aerosol and precursor emissions.

SST/SIE changes are the main driver of reduced cloud cover over North America and the North Atlantic. These reductions are consistent with reduced relative humidity and a weakened North Atlantic eddy-driven jet (Fig. 8a, b, c), which in turn, affects cloud cover and SSR over the North Atlantic by weakening storm track and reduced evaporation. The dipole pattern of zonal wind anomalies over North America in ERA5, with increases in zonal wind in the north and decreases in the south, and an associated reduction of relative humidity (Fig. 2), bear a similarity to the circulation and relative humidity changes in response to all forcings (Fig. 9). Circulation responses to AA (Fig. 7i) or to GHG are weak over North America (Fig. 3f). The response to SST/SIE also bear a similarity to changes in ERA5 reanalysis (Fig. 2), suggesting that observed changes in circulation and reduced relative humidity and cloud cover over North America might predominantly result from recent changes in SST/SIE (e.g., Seager and Hoerling 2014: Schubert et al. 2016). SST/SIE changes also lead to increases in the strength of the westerlies over Europe and decreases over the Mediterranean (Fig. 8c), associated with a reduction of cloud cover over southern Europe (Fig. 8a). The weakened North Atlantic eddy-driven jet is associated with weakened local meridional SST gradient (supplementary Fig. S1b) over the North Atlantic at about 45-50°N, suggesting a role of local SST changes (e.g., Baker et al. 2017). It is also associated with a northward shift of the Atlantic Intertropical Convergence Zone, enhanced precipitation over the Caribbean Sea (Fig. 8d), and a possible wave train from the Caribbean Sea to north-western Europe (Fig. 8e, f) (e.g., Cassou et al. 2005; Osborne et al. 2020).

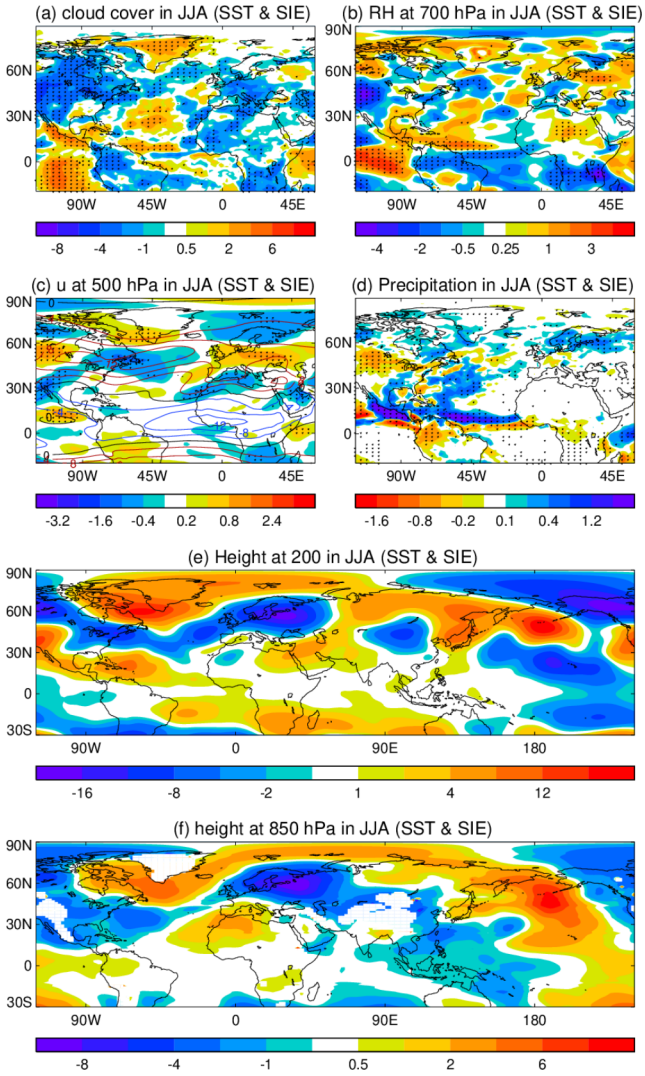

Fig. 8 Spatial patterns of changes in JJA for (a) cloud cover (%), (b) relative humidity at 700 hPa (%), (c) zonal wind at 500 hPa (m s^{-1}) with contours (red for westerlies and blue for easterlies) showing climatology in CON, (d) precipitation (mm day^{-1}), (e) eddy geopotential height (m) at 200 hPa, and (f) 850 hPa in response to SST/SIE changes (SST – CON). Dots in (a-d) highlight regions where differences are statistically significant at the 10% level based on a two-tailed Student's t-test

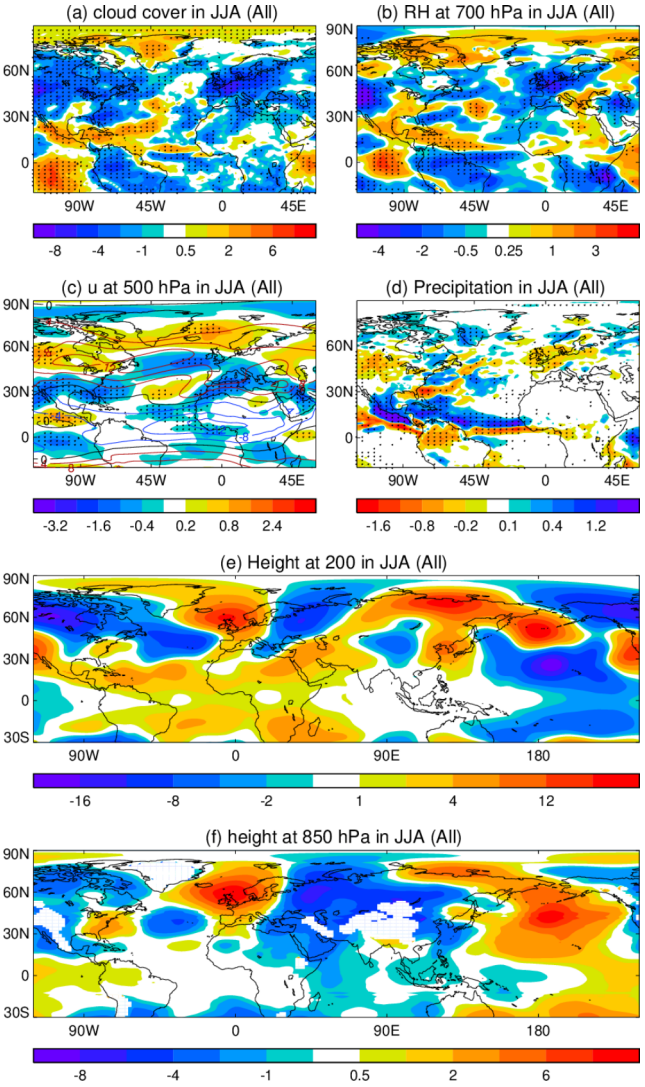

Fig. 9 Spatial patterns of changes in JJA for (a) cloud cover (%), (b) relative humidity at 700 hPa (%), (c) zonal wind at 500 hPa (m s^{-1}) with contours (red for westerlies and blue for easterlies) showing climatology in CON, (d) precipitation (mm day^{-1}), (e) eddy geopotential height (m) at 200 hPa, and (f) 850 hPa in JJA in response to all forcing changes (ALL – CON). Dots in (a-d) highlight regions where differences are statistically significant at he 10% level based on a two-tailed Student's t-test

3.2.5 Model biases in SSR and cloud cover

It is important to evaluate the model climatology as biases can potentially affect the simulated SSR and cloud cover response to external forcings. The model biases relative to ERA5 are illustrated in supplementary Fig. S3 and they show overestimations (by 10–30 Wm^{-2}) in SSR over land and underestimations (by 10–20 Wm^{-2}) over the North Atlantic along the North Atlantic eddy driven jet. Cloud cover biases are opposite to SSR biases and they show underestimations (4–10%) over land and overestimations (by 4–10%) over the North Atlantic, suggesting that model simulated SSR biases are partly related to cloud cover biases. Note these biases are larger than responses to different forcing factors together or separately. Although the model has these systematic biases over the North Atlantic sector in SSR and cloud cover, the responses to all forcings in model simulations for SSR and cloud cover shown in Sect. 3.2.1 and 3.2.2 gave similar changes as those in ERA5, especially over Europe and North America. The causes of these biases and how they may affect the model responses to external forcings are important questions but beyond the scope of this paper.

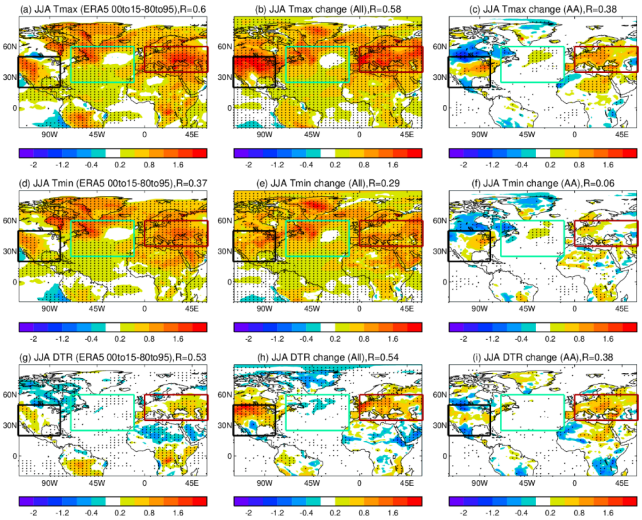

Fig. 10 Spatial patterns of changes in (a, b, c) daily maximum temperature (Tmax, °C), (d, e, f) daily minimum temperature (Tmin, °C), and (g, h, i) diurnal temperature range (DTR, °C) in JJA. (a, d, g) ERA5, (b, e, h) model responses to all forcings. (c, f, i) responses to aerosol emissions. Dots highlight regions where changes are statistically significant at 10% level based on the two-tailed Student's t-test. R in each panel is the pattern correlation between that variable and corresponding SSR changes over the whole domain shown in Fig. 2

3.3 Changes in summer mean daily maximum and minimum temperatures (tmax and tmin)

Changes of summer mean Tmax, Tmin, and diurnal temperature range (DTR) in ERA5 and model simulations are shown in Fig. 10. The ERA5 reanalysis shows large increases in both Tmax and Tmin over North America, Europe and a large part of the North Atlantic. The spatial patterns of changes in both Tmax and Tmin bear a similarity to the spatial pattern of changes in SSR with a pattern correlation of 0.60 and 0.37, respectively. However, the magnitude of changes in Tmax is larger (by 0.1-0.2ºC) over North America and Europe than those of Tmin, leading to increases of DTR over these two regions (Fig. 10g). Large changes of Tmax over North America and Europe and stronger pattern correlation between SSR and Tmax suggest that SSR changes have larger impacts on Tmax than Tmin, as would be expected.

In response to all forcings in model simulations, changes in both Tmax and Tmin are characterized by increases over North America, Europe, and the North Atlantic with the magnitude of Tmax changes being larger (by 0.3-0.4ºC) than changes in Tmin over North America and Europe with increases of DTR over the two regions (Fig. 10b, e, h). The pattern correlation between Tmax changes and SSR changes is 0.58 which is larger than the pattern correlation of 0.29 between Tmin and SSR. These features are similar to those in ERA5. However, the Tmax changes and DTR increases over North America and Europe are overestimated in response to all forcing changes when compared with those in ERA5 (Fig. 10). Aerosol changes lead to increases of Tmax over Europe but very weak changes in Tmin, leading to positive changes in DTR (Fig. 10c, f, i). This is consistent with the changes in SSR in the all forcing experiment over Europe being predominantly related to aerosol-induced SSR changes.

4 Seasonality of decadal changes in SSR and cloud cover in model simulations and in observations

The spatial patterns of four seasonal mean changes in SSR based on ERA5 and model responses to all forcings and AA forcing are shown in Fig. 11. The area averaged responses in SSR and cloud cover are shown in supplementary Fig. S4. These figures show a strong seasonality of changes in SSR and cloud cover, especially over Europe, with large changes in spring and summer and weaker changes in winter and autumn. Over Europe, the largest changes between 1980-1995 and 2000–2015 occur in summer with changes in spring showing similar features as those in summer with slightly weaker magnitudes (5–8 Wm^{-2}). However, changes in boreal autumn and winter are weaker. These seasonal changes give an annual mean change of SSR of about 4–5 Wm^{-2} in ISCCP and ERA5 over Europe between two periods which is similar to station observed changes of 5–6 Wm^{-2} in Potsdam, Germany, as documented in Wild (2016) and SSR trends over Europe of about 5 Wm^{-2} per decade over 1983–2010 in spring and summer, of 3 Wm^{-2} per decade in autumn and very weak trends in winter over Europe based on the Satellite Application Facility for Climate Monitoring (CM SAF) product documented in Sanchez-Lorenzo et al. (2017b). Over North America, the seasonal variation in the magnitude of the anomalies is smaller, but the smaller changes are again seen in autumn and winter compared to spring and summer.

The seasonal cycle of changes in SSR based on the satellite-derived product is reproduced well in model simulations in response to all forcings. Quantitatively, ERA5 gives a change of 10.0 and 6.1 Wm^{-2} (9.9 and 8.5 Wm^{-2} based on the ISCCP product) in summer (Fig. 3; Table 2) and spring (Fig. 11 and supplementary Fig. S4) over Europe. Model simulations also indicate that the strongest change in SSR over Europe occurs in summer (9.9 Wm^{-2}) with spring showing 6.0 Wm^{-2} and winter showing very weak changes (Fig. 11, supplementary Fig. S4). This seasonality of changes is predominantly due to the seasonality of clear sky SSR change in which the changes in AA play a primary role through both the seasonality of AOD changes (supplementary Fig. S5) and seasonality of incident solar radiation.

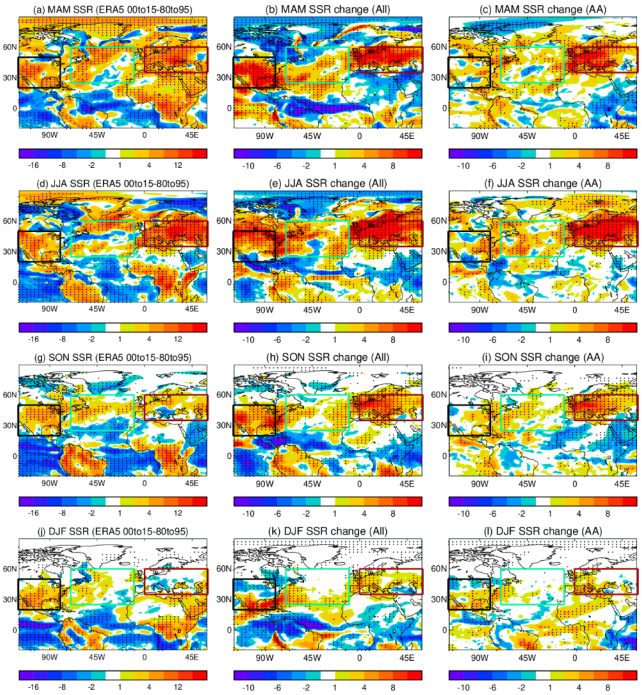

Fig. 11 Spatial patterns of changes in SSR (W m^{-2}) based on ERA5 (left column) for (a-c) MAM, (d-f) JJA, (g-i) SON, and (j-l) DJF in model responses to all forcings (middle column) and aerosol emissions (right column). Dots highlight regions where changes are statistically significant at the 10% level based on a two-tailed Student's t-test

The seasonality of AOD is mainly due to the dry seasons resulting in less wet deposition and favouring larger aerosol loads in the atmosphere since seasonality of emissions is weak. Large changes in SSR over North America also occurred in spring (8.7 and 4.8 Wm^{-2}) and summer (6.4 and 4.0 Wm^{-2}) between two periods based on ISCCP product and ERA5. The model responses give a change 8.1 Wm^{-2} in spring and 4.0 Wm^{-2} in summer (Fig. 11; Table 2, supplementary Fig. S4) and this seasonality of changes is predominantly the results of changes in cloud cover in response to changes in SST/SIE.

5 Conclusions

In this study, the observed characteristics of recent decadal changes in downward surface solar radiation (SSR) and cloud cover and their seasonality over the North Atlantic sector during the past four decades have been investigated. A set of atmospheric general circulation model experiments was carried out to explore potential drivers and assess the relative roles of different forcing factors in contributing to the changes observed between 1980-1995 and 2000–2015, and to elucidate the physical processes involved. The main findings are summarized as follows:

- Analyses of the time evolution of SSR and cloud cover, based on the ISCCP satellite-derived product and two reanalyses (ERA5 and NCEP2) show some consistent decadal trends over the North Atlantic sector in the last four decades despite large differences of climatological means among different data sets. These trends show a strong seasonality with the largest changes occurring in boreal summer and spring. The trends are characterized by increases in SSR over North America and Europe from 1980s to 2000s, accompanied by decreases in cloud cover.
- Timeslice experiments using the MetUM-GA6 AGCM reproduce many of the main features of the observed SSR and cloud cover changes over Europe and North America, including the seasonality of observed changes.
- Comparison of observed changes based on the satellite-derived product and reanalyses with model response to individual forcings indicates that recent decadal positive trends in SSR and negative trends in cloud cover over Europe are predominantly driven by AA emission changes. 71% of AA induced SSR changes is through aerosol-radiation interactions and 29% is through changes in cloud cover.
- Changes in AA, SST/SIE, and GHGs are all contributing factors to the model-simulated decadal positive trends in SSR and negative trends in cloud cover over North America of which changes in SST/SIE played the most important role.
- The seasonality of SSR changes between 1980-1995 and 2000–2015 over Europe is predominantly due to the seasonality of clear sky SSR change in which the changes in AA play a primary role. Seasonality of changes in SSR over North America in model simulations between two periods is mainly due to the seasonality of surface shortwave CRE changes, related to cloud cover changes in response to changes in SST/SIE.

The consistency between the modelled response to all forcing changes and the observed changes in SSR and cloud cover over the last four decades suggests that the observed changes over Europe and North America had a large forced component despite systematic biases in model climatologies. Responses to individual forcings indicate that the main drivers of SSR and cloud cover changes, and the physical processes involved, were different over North America and Europe. Over Europe, changes in aerosol emissions played a dominant role for recent decadal changes in SSR, with both the changes and their seasonality arising predominantly through aerosol radiation interactions. Meanwhile, changes in SST/SIE and GHGs play a secondary role, mainly through changes in cloud cover. In contrast, changes in AA, SST/SIE, and GHGs all contribute to model simulated SSR

increases and cloud decreases over North America, although the pattern and magnitude of the response is most strongly influenced by changes in SST/SIE.

Supplementary Information The online version contains supplementary material available at https://doi.org/10.1007/s00382-022-06438-3.

Acknowledgements This work was supported by the Natural Environment Research Council (NERC) North Atlantic Climate System Integrated Study (ACSIS) project. BD, RTS, and LJW are supported by the UK National Centre for Atmospheric Science, funded by the Natural Environment Research Council. We would like to thank two anonymous reviewers for their constructive comments and suggestions on the early version of this paper.

Author contributions BD conceived the study, performed model experiments and analysis, and wrote the first draft of the manuscript. All authors commented on previous versions of the manuscript, read and approved the final manuscript.

Funding This work was supported by the Natural Environment Research Council (NERC) North Atlantic Climate System Integrated Study (ACSIS) project. BD, RTS, and LJW are supported by the UK National Centre for Atmospheric Science, funded by the Natural Environment Research Council.

Data Availability The international satellite cloud climatology project (ISCCP) is available at https://isccp.giss.nasa.gov/. ERA5 reanalysis is available at https://climate.copernicus.eu/climate-reanalysis. NCEP II reanalysis is available at https://psl.noaa.gov/data/gridded/data.ncep.reanalysis2.html. Hadley Centre Sea Ice and Sea Surface Temperature data set (HadISST) is available at https://www.metoffice.gov.uk/hadobs/hadisst/. Model experiments and processed data are available upon request from the corresponding author BD (b.dong@reading.ac.uk).

Code Availability All analysis codes are available upon request from the corresponding author BD (b.dong@reading.ac.uk).

Declarations

Competing Interests The authors declare no competing interests.

References

Albrecht BA (1989) Aerosols, cloud microphysics, and fractional cloudiness. Science 245:1227–1230. https://www.science.org/doi/https://doi.org/10.1126/science.245.4923.1227

Allan R, Barlow M, Byrne MP, Cherchi A, Douville H, Fowler HJ, Gan TY, Pendergrass AG, Rosenfeld D, Swann ALS, Wilcox L, Zolina O (2020) Advances in understanding large-scale responses of the water cycle to climate change. Ann New York Acad Sci 1472:49–75. https://doi.org/10.1111/nyas.14337

Allen RJ, Norris JR, Wild M (2013) Evaluation of multidecadal variability in CMIP5 surface solar radiation and inferred underestimation of aerosol direct effects over Europe, China, Japan and India. J Geophys Res Atmos 118:6311–6336. https://doi.org/10.1002/jgrd.50426

Augustine JA, Dutton EG (2013) Variability of the surface radiation budget over the United States from 1996 through 2011 from high-quality measurements. J Geophy Res Atmos 118:43–53. doi:https://doi.org/10.1029/2012JD018551

Baker H, Woollings T, Mbengue C (2017) Eddy-driven jet sensitivity to diabetic heating in an idealized GCM. J Clim 30:6413–6431. https://doi.org/10.1175/JCLI-D-16-0864.1

Bellouin N, Rae J, Jones A, Johnson C, Haywood J, Boucher O (2011) Aerosol forcing in the climate model intercomparison project (CMIP5) simulations by HadGEM2-ES and the role of ammonium nitrate. J Geophys Res 116:D20206. https://doi.org/10.1029/2011JD016074

Bellouin N et al (2020) Bounding Global Aerosol Radiative Forcing of Climate Change. Rev Geophys 58. https://doi.org/10.1029/2019RG000660. e2019RG000660

Boers R, Brandsma T, Siebesma AP, (2017) https://doi.org/10.5194/acp-17-8081-2017

Boucher O et al (2013) Clouds and aerosols. In: Climate change 2013: the physical science basis. Contribution of Working Group I to the Fifth Assessment Report of the Intergovernmental Panel on Climate Change. Cambridge University Press, pp 571–657. doi:https://doi.org/10.1017/CBO9781107415324.016

Cassou C, Terray L, Phillips AS (2005) Tropical Atlantic influence on European heat waves. J Clim 18:2805–2811. https://doi.org/10.1175/JCLI3506.1

Cherian R, Quaas J (2020) Trends in AOD, clouds and cloud radiative effects in satellite data and CMIP5 and CMIP6 model simulations over aerosol source regions. Geophys Res Lett 47. https://doi.org/10.1029/2020GL087132. e2020GL087132

Christidis N, Jones GS, Stott PA (2015) Dramatically increasing chance of extremely hot summers since the 2003 European heatwave. Nat Clim Change 5:46–50. https://doi.org/10.1038/nclimate2468

Dong BW, Sutton RT, Shaffrey L, Wilcox L (2016) The 2015 European heat wave. Bull Am Meteorol Soc 97:S57–S62. https://doi.org/10.1175/BAMS-D-16-0140.1

Dong BW, Sutton RT, Shaffrey L (2017) Understanding the rapid summer warming and changes in temperature extremes since the mid-1990s over Western Europe. Clim Dyn 48:1537–1554

Dong BW, Sutton RT (2021) Recent trends in summer atmospheric circulation in the North Atlantic/European region: is there a role for anthropogenic aerosols? J Clim 34:6777–6795. doi: https://doi.org/10.1175/JCLI-D-20-0665.1

Folini D, Wild M (2011) Aerosol emissions and dimming/brightening in Europe: Sensitivity studies with ECHAM5-HAM. J Geophys Res 116:D21104. https://doi.org/10.1029/2011JD016227

Freychet N, Tett SFB, Bollasina M, Wang KC, Hegerl GC (2019) The local aerosol emission effect on surface shortwave radiation and temperatures. J Adv Model Earth Syst 11:806–817. https://doi.org/10.1029/2018MS001530

Gregory JM, Andrews T (2016) Variation in climate sensitivity and feedback parameters during the historical period. GeoPhys Res Lett 43:3911–3920. doi:https://doi.org/10.1002/2016GL068406

Hersbach H et al (2020) The ERA5 global reanalysis. Q J Roy Meteor Soc 146:1999–2049. https://doi.org/10.1002/qj.3803

Kanamitsu M, Ebisuzaki W, Woollen J, Yang SK, Hnilo JJ, Fiorino M, Potter GL (2002) NCEP-DOE AMIP-II reanalysis (R-2). Bull Am Meteorol Soc 83:1631–1644. https://doi.org/10.1175/BAMS-83-11-1631

Klimont Z, Smith SJ, Cofala J (2013) The last decade of global anthropogenic sulphur dioxide: 2000–2011 emissions. Environ Res Lett 8:014003. https://doi.org/10.1088/1748-9326/8/1/014003/meta

Lamarque J-F et al (2010) Historical (1850–2000) gridded anthropogenic and biomass burning emissions of reactive gases and aerosols: methodology and application. Atmos Chem Phys 10:7017–7039. https://doi.org/10.5194/acp-10-7017-2010

Lamarque J-F et al (2011) Global and regional evolution of short-lived radiatively-active gases and aerosols in the representative concentration pathways. Clim Change 109:191–212. https://doi.org/10.1007/s10584-011-0155-0

Luo F, Wilcox L, Dong B et al (2020) Projected near-term changes of temperature extremes in Europe and China under different aerosol emissions. Environ Res Lett 15:034013. https://doi.org/10.1088/1748-9326/ab6b34

Nabat P, Somot S, Mallet M, Sanchez-Lorenzo A, Wild M (2014) Contribution of anthropogenic sulfate aerosols to the changing Euro-Mediterranean climate since 1980. Geophys Res Lett 41:5605–5611. doi:https://doi.org/10.1002/2014GL060798

Norris JR, Wild M (2007) Trends in aerosol radiative effects over Europe inferred from observed cloud cover, solar 'dimming', and solar 'brightening'. J Geophys Res 112:D08214. https://doi.org/10.1029/2006JD007794

Norris JR, Evan AT (2015) Empirical Removal of Artifacts from the ISCCP and PATMOS-x Satellite Cloud Records. J Atmos Ocean Technol 32:691–702. https://doi.org/10.1175/JTECH-D-14-00058.1

Norris JR, Allen RJ, Evan AT, Zelinka MD, O'Dell CW, Klein SA (2016) Evidence for climate change in the satellite cloud record. Nature 536:72–75. https://doi.org/10.1038/nature18273

Osborne JM, Collins M, Screen JA, Thomson SI, Dunstone N (2020) The North Atlantic as a driver of summer atmospheric circulation. J Clim 33:7335–7351. https://doi.org/10.1175/JCLI-D-19-0423.1

Otto FEL, Massey N, van Oldenborgh GJ, Jones R, Allen MR (2012) Reconciling two approaches to attribution of the 2010 Russian heatwave. Geophys Res Lett 39:L04702. https://doi.org/10.1029/2011GL050422

Pfeifroth U et al (2018a) Satellite-based trends of solar radiation and cloud parameters in Europe. Adv Sci Res 15:31–37. https://doi.org/10.5194/asr-15-31-2018

Pfeifroth U et al (2018b) Trends and variability of surface solar radiation in Europe based on surface- and satellite-based data records. J Geophys Res Atmos 123:1735–1754. https://doi.org/10.1002/2017JD027418

Ramanathan V, Cess R, Harrison E, Minnis P, Barkstrom B et al (1989) Cloud-radiative forcing and climate: results from the earth radiation budget experiment. Science 243:57–63. DOI: https://doi.org/10.1126/science.243.4887.57

Rayner NA, Parker DE, Horton EB, Folland CK, Alexander LV, Rowell DP, Kent EC, Kaplan A (2003) Global analyses of SST, sea ice and night marine air temperature since the late nineteenth century. J Geophys Res 108:4407. https://doi.org/10.1029/2002JD002670

Ruckstuhl C, Norris J (2009) How do aerosol histories affect solar "dimming" and "brightening" over Europe? IPCC-AR4 models versus observations. J Geophys Res 114:D00D04. doi:https://doi.org/10.1029/2008JD011066

Sanchez-Lorenzo A, Enriquez-Alonso A, Calbó J, González JA, Wild M, Folini D, Norris JR, Vicente-Serrano SM (2017a) Fewer clouds in the Mediterranean: consistency of observations and climate simulations. Sci Rep 7:1–10. https://doi.org/10.1038/srep41475

Sanchez-Lorenzo A, Vicente-Serrano SM, Wild M et al (2017b) Trends in downward surface solar radiation from satellites and ground observations over Europe during (1983–2010). Remote Sens Environ 189:108–117. DOI:https://doi.org/10.1016/j.rse.2016.11.018

Schubert SD et al (2016) Global meteorological drought: a synthesis of current understanding with a focus on SST drivers of precipitation deficits. J Clim 29:3989–4019. https://doi.org/10.1175/JCLI-D-15-0452.1

Schwarz M, Folini D, Yang S, Allan RP, Wild M (2020) Changes in atmospheric shortwave absorption as important driver of dimming and brightening. Nat Geosci 13:8. https://doi.org/10.1038/s41561-019-0528-y

Seager R, Hoerling M (2014) Atmosphere and ocean origins of North American droughts. J Clim 27:4581–4606. https://doi.org/10.1175/JCLI-D-13-00329.1

Smith TT, Zaitchik BF, Gohlke JM (2013) Heat waves in the United States: definitions, patterns and trends. Clim Change 118:811–825. doi: https://doi.org/10.1007/s10584-012-0659-2

Stephens GL, Li J, Wild M et al (2012) An update on Earth's energy balance in light of the latest global observations. Nat Geosci 5:691–696. https://doi.org/10.1038/ngeo1580

Stjern CW, Kristjansson JE, Hansen AW (2009) Global dimming and global brightening—an analysis of surface radiation and cloud cover data in northern Europe. Int J Climatol 29:643–653. https://doi.org/10.1002/joc.1735

Tang T, Shindell D, Zhang Y, Voulgarakis A, Lamarque J-F, Myhre G, Stjern CW, Faluvegi G, Samset BH (2020) Response of shortwave cloud radiative effect to greenhouse gases and aerosols and its impact on daily maximum temperature. Atmos Chem Phys 20:8251–8266. https://doi.org/10.5194/acp-20-8251-2020

Turnock ST et al (2015) Modelled and observed changes in aerosols and surface solar radiation over Europe between 1960 and 2009. Atmos Chem Phys 15:9477–9500. https://doi.org/10.5194/acp-15-9477-2015

Yang Y et al (2018a) Recent intensification of winter haze in China linked to foreign emissions and meteorology. Sci Rep 8:2107. https://doi.org/10.1038/s41598-018-20437-7.

Yang Y et al (2018b) Source apportionments of aerosols and their direct radiative forcing and long-term trends over continental United States. Earths Future 6:793–808. https://doi.org/10.1029/2018EF000859

Yang Y, Lou S, Wang H, Wang P, Liao H (2020) Trends and source apportionment of aerosols in Europe during 1980–2018. Atmos Chem Phys 20:2579–2590. https://doi.org/10.5194/acp-20-2579-2020.

Walters D et al (2017) The Met Office unified model global atmosphere 6.0/6.1 and JULES global land 6.0/6.1 configurations. Geosci Model Dev 10:1487–1520. https://doi.org/10.5194/gmd-10-1487-2017

Wang Z, Zhang M, Wang L, Qin W (2022) A comprehensive research on the global all-sky surface solar radiation and its driving factors during 1980–2019. Atmos Res 265:105870. https://doi.org/10.1016/j.atmosres.2021.105870

Wild M et al (2005) From Dimming to Brightening: Decadal Changes in Solar Radiation at Earth's Surface. Science 308:847–850. DOI: https://doi.org/10.1126/science.1103215

Wild M (2016) Decadal changes in radiative fluxes at land and ocean surfaces and their relevance for global warming. Wiley Interdiscip Rev Clim Change 7:91–107. https://doi.org/10.1002/wcc.372

Wohland J, Brayshaw DJ, Bloomfield H, Wild M (2020) European multidecadal solar variability badly captured in all centennial reanalyses except CERA20C. Environ Res Lett 15:104021. https://doi.org/10.1088/1748-9326/aba7e6

Zhou C, Zelinka MD, Klein SA (2016) Impact of decadal cloud variations on the Earth's energy budget. Nat Geosci. https://doi.org/10.1038/NGEO2828

Zhou C, Zelinka MD, Klein SA (2016) Impact of decadal cloud variations on the Earth's energy budget. Nat Geosci. https://doi.org/10.1038/NGEO2828